EXPERIMENTAL AND NUMERICAL ANALYSIS OF FORCED CONVECTION IN A TWISTED TUBE

by

Suvanjan BHATTACHARYYA[a,], Ali Cemal BENIM[b,c], Himadri CHATTOPADHYAY[d], and Arnab BANERJEE[e]*

[a]Department of Mechanical and Aeronautical Engineering, University of Pretoria, Hatfield, Pretoria, South Africa
[b]Center of Flow Simulation, Deparment of Mechanical and Process Engineering, Duesseldorf University of Applied Sciences, Duesseldorf, Germany
[c]Institute of Thermal Power Engineering, Department of Mechanical Engineering, Cracow University of Technology, Cracow, Poland
[d]Department of Mechanical Engineering, Jadavpur University, Kolkata, West Bengal, India
[e]Department of Mechanical Engineering, MCKV Institute of Engineering, Howrah, West Bengal, India

In the present paper, along with experimental study, CFD analysis of forced convection in a twisted tube is performed, using the transition SST model which can predict the change of flow regime from laminar through transition to turbulent. The differential governing equations are discretized by the finite volume method. The investigations are conducted for Reynolds numbers ranging from 100 to 50000 covering laminar, transitional and turbulent regimes, and for three length and three pitch ratios. The predictions are observed to show a good agreement with the measurements and published correlations of other authors. The analysis indicates that the large length ratio and small pitch ratio yields a higher heat transfer rate with relatively low performance penalty. The transition from laminar to turbulent regime is observed between Reynolds numbers of 2500 to 3500 for all cases. For almost all investigated cases the performance factors are greater than unity.

Key words*: turbulent forced convection, twisted tube, swirl flow, heat transfer enhancement*

Introduction

Heat exchanger is a device facilitating heat transfer between two or more fluids [1]. It is used in a vast number of industrial applications, such as thermal power plants, chemical processing plants, air conditioning equipment, refrigerators, radiator for space vehicles as well as automobiles, extending up to micro-scale applications [2, 3]. Obviously, for improving the efficiency of energy utilization, enhancement of heat transfer in such applications plays an important role. To this goal, two techniques can generally be identified, namely, the active and passive techniques. Active techniques include surface vibration, fluid vibration, *etc.* for

---
* Corresponding author, e-mail: suvanjanmechanical@gmail.com

increasing heat transfer [4]. In passive techniques, the applied methods usually involve a modification of the channel geometry to enhance heat transfer. A special category herein is the use of bluff bodies that increase heat transfer by vortex shedding [5, 6]. Passive methods also include different arrangements, such as impinging jet [7, 8] instead of wall-parallel flow.

A passive technique that attracted considerable attention is the insertion of structures such as twisted tapes that induce a swirling motion. Indeed, industrial heat transfer equipment's are generally operated in turbulent/swirl flow conditions where their performance in terms of energy transfer rate is high, compared with laminar flow by virtue of the high degree of turbulence in turbulent swirl flow.

Heat transfer characteristics under transitional flow conditions in most of thermal problems are of considerable interest. Predicting transition of laminar regime to turbulent in heat transfer augmentation techniques will be highly useful to design any heat transfer equipment. There is constant thrive in the studies on transition from laminar to turbulent flow.

Many researchers performed surveys on passive enhancement method of this kind, which were very inspiring, such as channel with a cylinder roughness [9] and compound heat transfer enhancement of a convergent-divergent tube with a twisted tape [10]. Swirling flow may increase the heat transfer through the boundary-layer by interruption or thinning and also increase the turbulence levels considerably [11]. Tube with wire coil inserts [12] can generate vortex and also can develop secondary flow.

Tube insert technology – *i. e*., insertion of tape inside a channel - was used in some previous work. Bhattacharyya *et al*. [13, 14] and Saha *et al*. [15] studied, experimentally, center-clearing twisted tapes with artificial rib roughness and achieved considerable improvement. Meng *et al*. [16] performed experiments on elliptical tube type swirl generator. Some earlier research [17, 18] showed that vortex geometry may affect heat transfer which can be utilized to design heat exchangers. Chen *et al*. [19] studied experimentally heat transfer augmentation techniques of a dimpled tube. Vicente *et al*. [20] reported on thermohydraulic performance of helically dimpled tubes for laminar and transition flow. Mengna *et al*. [21] studied compound heat transfer enhancement of a converging-diverging tube with swirl generator inserts. Sivashanmugam *et al*. [22] reported on experiments on thermohydraulic characteristics of laminar stream in circular channel fitted with screw type tape. Additional information on similar vortex originator may be acquired from [23-27].

In the present paper, a numerical and experimental study of forced convection in circular twisted tube is presented. Air is used as working medium. At the prevailing relatively small/moderate temperature differentials, constant material properties are assumed. A sketch of the device is presented in fig. 1, where the circular twisted enhancers can be recognized.
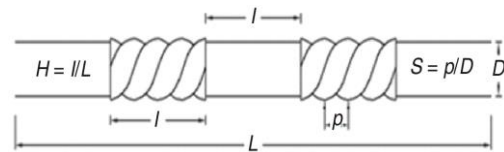

Figure 1. Sketch of geometry

Experimental

Figure 2 demonstrates the schematic figure of the experimental set-up. The working medium, atmospheric air, is sucked by a 7.0 kW blower, which flows through a PVC pipe and finally a rotameter. The latter is used to measure the flow rate (range: 120-520 LPH, error: 0.0442%). A bypass valve is installed between the blower and the rotameter to control the flow rate. For measuring the pressure drop across the tube, two pressure taps are placed at inlet and outlet of the test section. A U-tube manometer (range: 1-150 mm Hg) is, then, used
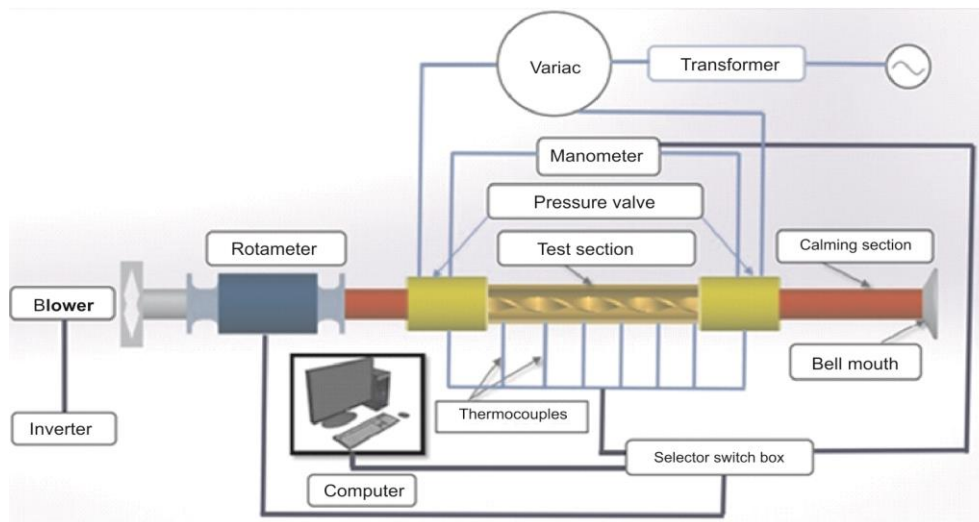
Figure 2. Schematic of experimental set-up

to measure the pressure drop. A total of 28 thermocouples are fitted on the tube outside wall by brazing at 7 equidistant axial locations, each position containing 4 thermocouples equidistantly distributed along the circumference. The inner wall temperatures are obtained from the measured heat-flow rate and the thermal resistance of the wall, assuming 1-D heat conduction across the wall. The test section is electrically heated up by nichrome heater wire providing essentially uniform wall heat flux. Porcelain bead types of insulation are used on nichrome heater wire, with no direct interaction of the nichrome heater wire with the tube wall. A 1.5 KW variac is used in which the variations of voltage and current are 10.0-30.0 V and 1.0-3.0 A, respectively (error: 0.072% in the current and voltage compared to the nominal value). In order to minimize the heat loss, the tube is insulated using glass-wool layers. During the experiments, the heat loss to surroundings has been quantified. The heat equilibrium test has shown that the heat absorbed by air to be 2-3% lower than the heat supplied by the electrical winding. The uncertainty in Reynolds number, friction factor and Nusselt number are estimated as $\pm4.17\%$, $\pm 6.66\%$, and $\pm7.42\%$, respectively, following the procedure of Bhattacharyya *et al*. [13].

Carrying out the experiments, the set-up is, first, allowed to avail steady-state by providing sufficient time, which was about two hours. When the standard deviations of the temperature and mass-flow rate were less than 0.03 $^{\circ}$C and 0.011 kg/s, respectively, a steady-state was assumed to be reached.

A circular tube having 22 mm inside diameter and length of 2.0 m is used for the experiment purpose. The tube as depicted in fig. 1 is made out of brass. For validation purpose the experiment is executed in a smooth tube and then for twisted tubes for three different length ratios ($H = l/L = 0.2$, 0.25 and 0.30), and three different pitch ratios ($S = p/d = 0.22$, 0.36, and 0.45).

Modelling

Steady-state, incompressible flow of a Newtonian fluid with constant material properties and negligible buoyancy are assumed. Obviously, the radiative heat transfer does either not play a role in the present application at low temperatures with a practically non-

S1046

Bhattacharyya, S., *et al.*: Experimental and Numerical Analysis of Forced …
THERMAL SCIENCE: Year 2019, Vol. 23, Suppl. 4, pp. S1043-S1052

participating medium [28]. The turbulence is modelled within RANS applying a turbulent viscosity model, in particular, the transitional SST model of turbulence of Menter [see 29], which was successfully used, previously, in various applications in fluids and thermal engineering [30-34]. Oclon *et al*. [32] used this model for heat transfer predictions in conjunction with the prediction of fouling in fin-and-tube heat exchanger, whereas Kadiyala and Chattopadhyay [34] applied the model for studying the effects of cooling jets on moving surface. The computational modelling is performed based on the general-purpose CFD solver ANSYS Fluent [29]. For a detailed description of the model and for the model equations, the reader may refer to [29].

At the inlet boundary, all dependent variables are prescribed. For the turbulence quantities, a turbulence intensity of 5% and a macro-length scale equal to the tube diameter is assumed to derive the boundary conditions. This may be seen inappropriate for low Reynolds numbers that indicate a laminar flow. However Abraham *et al*. [31] showed that the applied transitional SST model can cope with this situation, predicting a rapid drop of the viscosity to the molecular value, if the flow is laminar, so that the results are not affected. At the outlet, a zero-gradient boundary condition applied for all convective-diffusively transported variables, along with a constant static pressure. At walls, the no-slip boundary conditions apply, where the wall temperature is prescribed. As far as the near-wall turbulence is concerned, no wall-functions [29] are used, as the applied turbulence model can cope with low Reynolds number, transitional turbulence.

The velocity-pressure coupling is treated by the Semi Implicit Pressure Linked Equations (SIMPLE) scheme [29]. For discretizing the convective terms, a second order accurate upwind scheme [29] is used. The discretized equations are then solved iteratively in double precision solver. The convergence criteria for continuity, momentum and energy are set at 10^{-4}, 10^{-5}, and 10^{-7}, respectively. The convergence criterion for the four turbulence quantities was fixed at 10^{-4}.

Data reduction

The bulk fluid temperature, T_b, is calculated as the arithmetic average of the fluid and inlet, T_i, outlet, T_o, temperatures. The wall heat flux, q_w, is deduced from the difference in the energy flow rates of the inflowing and outflowing fluids. The heat transfer coefficient, h, [1] is obtained from:

$$h = \frac{q_w}{T_w - T_b} \tag{1}$$

where the wall temperature, T_w, is obtained as the arithmetic average of the wall temperatures measured by the 28 thermocouples. The Nusselt number is obtained from:

$$Nu = \frac{hD}{k} \tag{2}$$

where k denotes the fluid thermal conductivity and D the diameter of the plain tube. The Darcy friction factor, f, is evaluated from:

$$f = \frac{\Delta p}{\frac{L}{D} \frac{1}{2} \rho U^2} \tag{3}$$

Bhattacharyya, S., *et al.*: Experimental and Numerical Analysis of Forced …
THERMAL SCIENCE: Year 2019, Vol. 23, Suppl. 4, pp. S1043-S1052

S1047

In the previous equation, Δp denotes the pressure drop across the tube, U – the axial bulk velocity for the plain tube, ρ – the density, and L – the tube length. The Reynolds number is also defined based on D and U. The air material properties are evaluated at the bulk fluid temperature, T_b.

To evaluate the effect of heat transfer enhancement under given pumping power, the thermohydraulic performance factor, η, [35-37] is used, where the subscript 0 refers to the smooth tube:

$$\eta = \frac{\dfrac{Nu}{Nu_0}}{\left(\dfrac{f}{f_0}\right)^{0.33}} \tag{4}$$

Results and discussion

An unstructured grid with non-uniform grid density distribution was created. A grid independence study was performed, where the basic parameters such as the Nusselt number and friction factor were obtained and compared on three different grids, the results of which are shown in tab. 1, for the case with Re = 10000, H = 0.30, S = 0.22. The Grid 1 consisting of 777235 nodes, which seems to provide sufficient accuracy, is used for the present computations. Different views of the surface grid are provided in fig. 3.

Table 1. Grid independence study (Re = 10000, H = 0.30, S = 0.22)

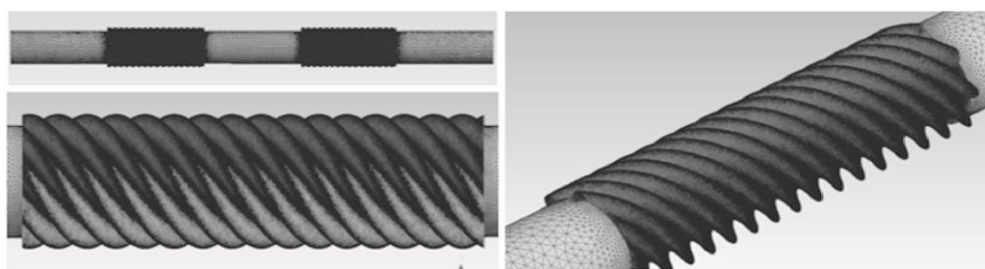|	Total number of nodes	Nusselt number	f
Grid 1	777235	49.14	0.046
Grid 2	814887	49.12	0.047
Grid 3	1000112	49.12	0.047

Figure 3. Views of grid

Figures 4(a) and 4(b) show the assessment for the Nusselt number and friction penalties, for a plain tube. Here, the results are compared with the empirical correlations by Dittus-Boelter [1] for the Nusselt number, and with the correlation of Blasius [1] for the friction factor in the turbulent region (Re > 5000), wheras, in the laminar region (Re < 2000), the analytical expressions known for the laminar flow (Nu = 3.66 and f = 64/Re) are used for the comparison. On the whole, the relative errors are quite small, indicating that there is a wonderful agreement between the investigational data and those forecasted by the standard correlations for the plain tube. The results prove the reliability of the experimental and numerical procedures for predicting fluid-flow and heat transfer characteristics.

The numerically (num.) and experimentally (exp.) obtained Nusselt numbers for the tube with twisted geometry, for certain values of the length ratio, H ($H = l/L$), and the pitch

S1048

Bhattacharyya, S., *et al.*: Experimental and Numerical Analysis of Forced …
THERMAL SCIENCE: Year 2019, Vol. 23, Suppl. 4, pp. S1043-S1052

ratio, S ($S = p/D$), are presented in fig. 5, as function of Reynolds number (see fig. 1, for the definitions of H and S).
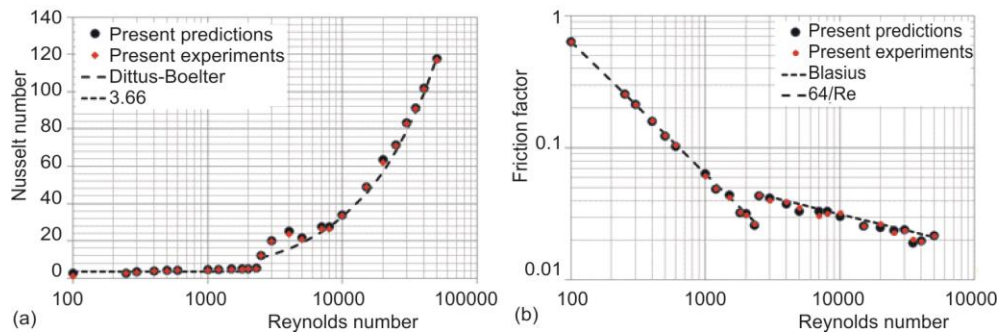

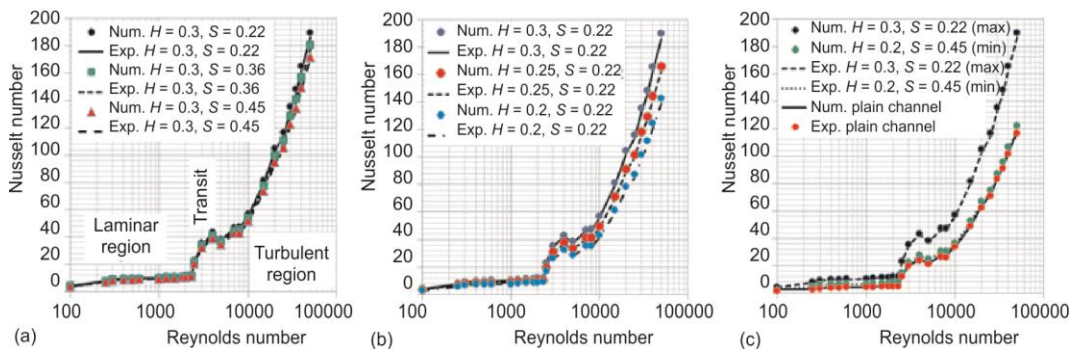**Figure 4. Plain tube, (a) Nusselt number, (b) friction factor**

Figure 5. Nusselt number variation with Reynolds number; (a) varying *S* with constant *H*,
(b) varying *H* with constant *S*, (c) minimum and maximum values (*for colour image see journal web site*)

As expected, Nusselt number increases with increasing Reynolds number for all cases. In fig. 5(a), cases with different $S = 0.22$, 0.36, and 0.45 are compared while $H = 0.3$ remains constant. One can observe that the small values of S lead to increased Nusselt numbers. Laminar, turbulent and transitional regions are also indicated in the figure, which show different characteristics. Figure 5(b) compares the effect of H by considering its three values (0.2, 0.25, and 0.3) while keeping $S = 0.22$ constant. It is observed that larger values of H lead to higher Nusselt numbers and this effect, fig. 5(b), is even stronger than the one observed for decreasing S, fig. 5(a). The minimum and maximum increases of the Nusselt number are observed for the smallest S and largest H ($H = 0.2$, $S = 0.45$) and the largest H and smallest S ($H = 0.3$, $S = 0.22$), respectively. These cases are compared with the results for the plain tube in fig. 5(c). One can see the case $H = 0.2$, $S = 0.45$ provides only a marginal increase of the Nusselt number compared to the plain tube, while for the case $H = 0.3$, $S = 0.22$ a remarkable increase, which is around 50%, is observed. One can also see that the agreement between the predictions and experiments is very good, for all considered cases, fig. 5.

Figure 6 shows the Num. and Exp. obtained variations of the friction factor with the Reynolds number. It can be viewed that the friction factor decreases with increasing Reynolds number, for all cases. Figures 6(a) and 6(b) demonstrate the effect of the pitch ratio (varying S with constant H) and length ratio (varying H with constant S), respectively. One can see that

Bhattacharyya, S., *et al.*: Experimental and Numerical Analysis of Forced …
THERMAL SCIENCE: Year 2019, Vol. 23, Suppl. 4, pp. S1043-S1052

S1049

the friction factor increases with decreasing S and increasing H. The minimum and maximum increase of the friction factor is observed for the smallest S and largest H ($H = 0.2$, $S = 0.45$) and the largest H and smallest S ($H = 0.3$, $S = 0.22$), respectively. These cases are compared with the results for the plain tube in fig. 6(c). One can see the case $H = 0.2$, $S = 0.45$ has a considerable increase compared to the plain tube, while for the case $H = 0.3$, $S = 0.22$, only a marginal further increase is observed, except for low Reynolds numbers. One can also see that the agreement between the predictions and experiments is very good for all cases, fig. 6.
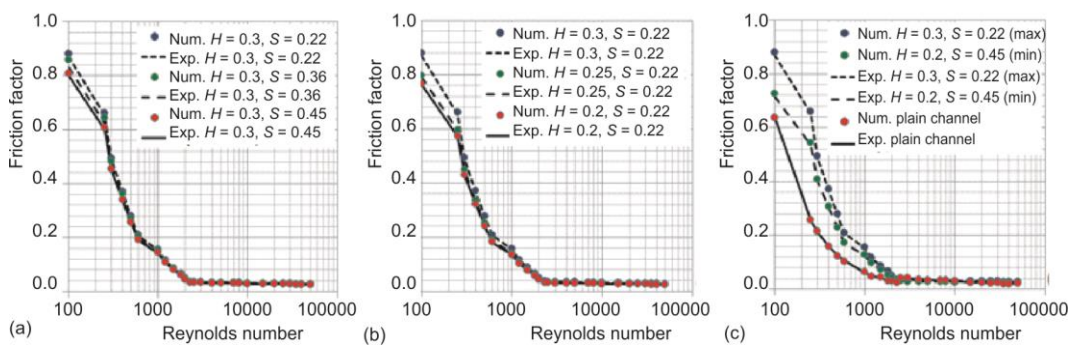

Figure 6. Friction factor variation with Reynolds number; (a) varying S with constant H, (b) varying H with constant S, (c) minimum and maximum values (*for colour image see journal web site*)

Distribution of the dimensionless velocity magnitude (non-dimensionalized by the inlet velocity) is shown in fig. 7, for the case with Re = 10000, $H = 0.3$, and $S = 0.22$. Figure 7(a) shows the distribution in a longitudinal plane, whereas cross-sectional planes along the length of the tube are displayed in fig. 7(b). It can be witnessed that twisted geometry has solid impact over the flow field. In the twisted parts, the velocity in the central regions increases considerably due to the displacement effect caused by the twist structure acting like roughness, whereas an additional contribution results by the generated swirl component.
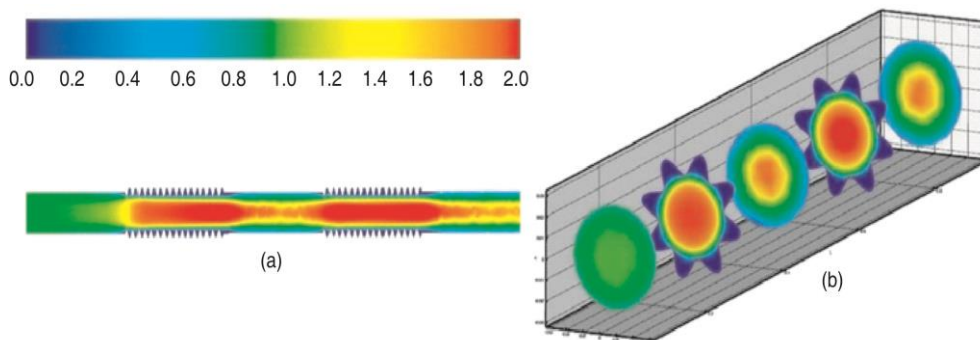

Figure 7. Dimensionless velocity contours; (a) axial plane, (b) transverse planes

Figures 8 shows the distribution of dimensionless temperature based on the wall, T_w, and inlet, T_{in}, temperatures, $(T - T_{in})/(T_w - T_{in})$, for Re = 10000 for the twisted tube with $H = 0.3$ and $S = 0.22$. Figure 8(a) shows the distribution in a longitudinal plane and fig. 8(b) shows distributions in cross-sectional planes along the length of the tube. One can see from the figure that there is a change in the temperature field throughout the tube. This shows that

S1050

Bhattacharyya, S., *et al.*: Experimental and Numerical Analysis of Forced …
THERMAL SCIENCE: Year 2019, Vol. 23, Suppl. 4, pp. S1043-S1052

the turbulator (twisted geometry) can offer a significant effect on the temperature field, since it can induce better mixing of the fluid between the boundary layer and the core flow.
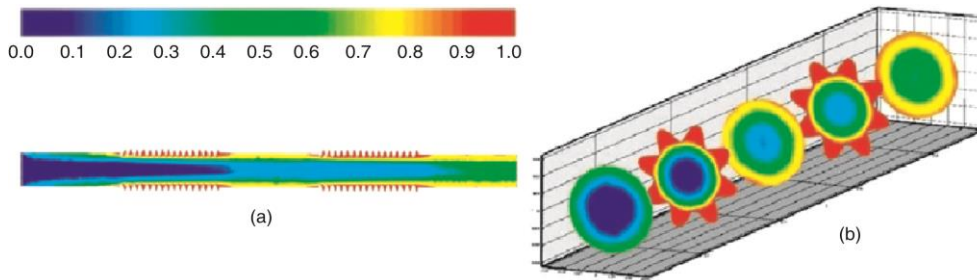

Figure 8. Dimensionless temperature contours; (a) axial plane, (b) transverse planes

In general, the thermal effectiveness of heat exchangers is evaluated based on the enhancement of convective heat transfer coefficient and reduction of power consumption to pump the fluid through the device. In the present study, the thermal performance is assessed by comparing the convective heat transfer coefficients of the enhanced and reference heat transfer surfaces for the same pumping power.

Figure 9 shows the variations of the thermal performance factor with Reynolds number for the twisted tube. It can be distinguished that the thermal performance factor is more than unity for most of the time with varying Reynolds number. At higher Reynolds numbers (Re = 35000-50000) for the case of $H = 0.2$ and $S = 0.45$, the thermal performance factor decreases to a value less than 1.0. If $\eta \geq 1.0$, this indicates that the heat-flow rate for the tube with twisted geometry is higher than that for the plain tube at the same pumping power. Figure 9 also shows that the thermal performance factor of the tube with twisted geometry increases with an increase of length ratio ($H = l/L$) and decrease in pitch ratio ($S = p/d$). The highest thermal performance factor is obtained for tube with $H = 0.3$ and $S = 0.22$. The lowest thermal performance factor is obtained for the tube with $H = 0.2$ and $S = 0.45$.
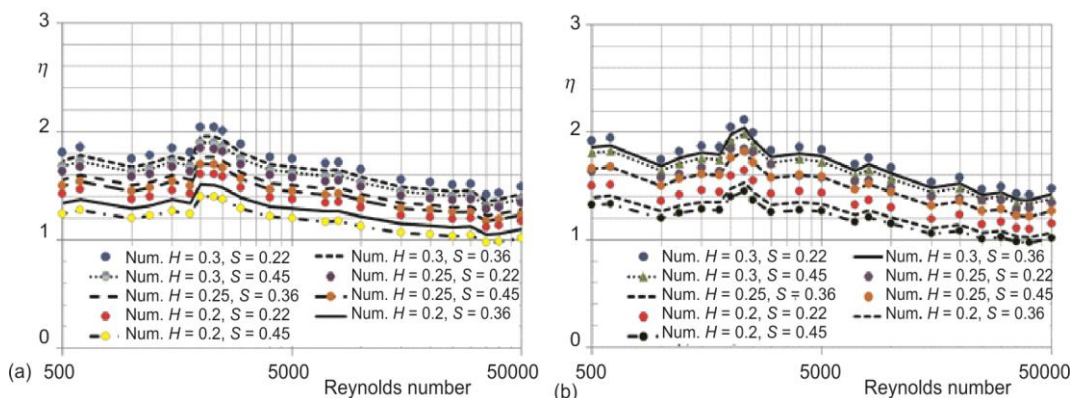

Figure 9. Thermal exhancement factor; (a) predictions, (b) experiments
(*for colour image see journal web site*)

For a better overview, the experimentally and numerically obtained maximum ($H = 0.3$, $S = 0.22$) and minimum ($H = 0.2$, $S = 0.45$) performance factors are presented,
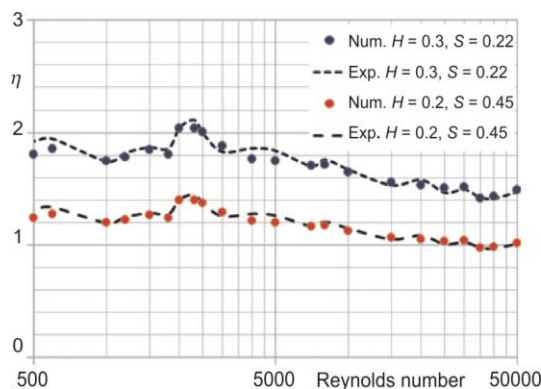
Bhattacharyya, S., *et al.*: Experimental and Numerical Analysis of Forced …
THERMAL SCIENCE: Year 2019, Vol. 23, Suppl. 4, pp. S1043-S1052

S1051

Figure 10. Thermal enhancement factor, comparison between predictions and experiments for the lowest and highest values

again, in fig. 10. It can again be observed that a certain improvement in the thermal performance is obtained for almost all configurations, within the range 1.0-2.0. approximately.

Conclusions

In this work, the heat transfer and fluid-flow characteristics of turbulent flow through a heat exchanger mounted with circular twisted tube were investigated experimentally and numerically. It is observed that the twisted geometry enhances heat transfer considerably. Heat transfer also increases with an increase of length ratio and decrease in pitch ratio. The twisted geometry with the large length ratio and small pitch ratio leads to the highest heat transfer augmentation, where the Nusselt number is higher by approximately 50% on the average, compared with that of the plain tube. The friction factor decreases as the Reynolds number increases, but increases with an increase in the length ratio and decrease in pitch ratio. In spite of the high friction penalty, the case with $H = 0.3$ and $S = 0.22$ yields the maximum thermal performance factor, with a value of approximately 2.0, on the average.

References

[1] Shah, K. R., Sekulic, D. P., *Fundamentals of Heat Exchanger Design*, Wiley, Chichester, UK, 2003
[2] Maqableh, A. M., *et al.*, Heat Transfer Characteristics of Parallel and Counter Flow Micro-Channel Heat Exchangers with Varying Wall Resistance, *Progress in Computational Fluid Dynamics – An International Journal*, *11* (2011), 5, pp. 318-328
[3] Ebling, D. G., *et al.*, Development of a System for Thermoelectric Heat Recovery From Stationary Industrial Processes, *Journal of Electronic Materials*, *45* (2016), 7, pp. 3433-3439
[4] Benim, A. C., *et al.*, Computational Analysis of Transient Heat Transfer in Turbulent Pipe Flow, *International Journal of Thermal Sciences, 43* (2004), 8, pp. 725-732
[5] Benim, A. C., *et al.*, Computational Analysis of Turbulent Forced Convection in a Channel with a Triangular Prism, *International Journal of Thermal Sciences, 50 (2011)*, 10, pp. 1973-1983
[6] Taymaz, I., *et al.*, Numerical Investigation of Incompressible Fluid Flow and Heat Transfer Across a Bluff Body in a Channel Flow, *Thermal Science, 19* (2015), 2, pp. 537-547
[7] Chattopadhyay, H., Benim, A. C., Turbulent Heat Transfer over a Moving Surface Due to Impinging Slot Jets, *Journal of Heat Transfer – Transactions of the ASME, 133* (2011), 10, 104502
[8] Benim, A. C., *et al.*, Computational Investigation of Turbulent Jet Impinging onto Rotating Disk*, International Journal of Numerical Methods for Heat & Fluid-flow, 17* (2007), 3, pp. 284-301
[9] Mahir, N., Altac, Z., Numerical Investigation of Flow and Heat Transfer Characteristics of Two Tandem Circular Cylinders of Different Diameters, *Heat Transfer Engineering, 38* (2016), 16, pp. 1367-1381
[10] Hong, M., *et al.*, Compound Heat Transfer Enhancement of a Convergent-Divergent Tube with Evenly Spaced Twisted Tapes, *Chinese J. Chemical Engineering, 15* (2007), 6, pp. 814-820
[11] Benim, A. C., *et al.*, Experimental and Numerical Investigation of Isothermal Flow in an Idealized Swirl Combustor, *Int. Journal of Numerical Methods for Heat & Fluid Flow, 20* (2010)*,* 3, pp. 348-370
[12] Rout, P. K., Saha, S. K., Laminar Flow Heat Transfer and Pressure Drop in a Circular Tube Having Wire-Coil and Helical Screw-Tape Inserts, *Journal of Heat Transfer*, *135* (2013), 2, 021901
[13] Bhattacharyya, S., *et al.*, Laminar Flow Heat Transfer Enhancement in a Circular Tube Having Integral Transverse Rib Roughness and Fitted with Centre-Cleared Twisted-Tape, *Experimental and Thermal Fluid Science, 44* (2013), 2., pp., 727-735

S1052

Bhattacharyya, S., *et al.*: Experimental and Numerical Analysis of Forced ...
THERMAL SCIENCE: Year 2019, Vol. 23, Suppl. 4, pp. S1043-S1052

[14] Bhattacharyya, S., Saha, S. K., Thermohydraulics of Laminar Flow through a Circular Duct Having Integral Helical Rib Roughness and Fitted with Centre-Cleared Twisted-Tape, *Experimental Thermal and Fluid Science, 42* (2012), Oct., pp. 154-162

[15] Saha, S. K., *et al.*, Thermohydraulics of Laminar Flow of Viscous Oil Through a Circular Tube Having Integral Axial Rib Roughness and Fitted with Centre-Cleared Twisted-Tape, *Experimental and Thermal Fluid Science, 41* (2012), Sept., pp. 121-129

[16] Meng, J. A, *et al.*, Experimental Study on Convective Heat Transfer in Alternating Elliptical Axis Tubes, *Experimental Thermal and Fluid Science, 29* (2005), 4, pp. 457-465

[17] Saha, S. K., Thermohydraulics of Laminar Flow through Rectangular and Square Ducts with Axial Corrugation Roughness and Twisted Tapes with Oblique Teeth, *ASME Journal Heat Transfer, 132* (2010), 8, 081701

[18] Mwesigye, A., *et al.*, Heat Transfer and Entropy Generation in a Parabolic Trough Receiver with Wall-Detached Twisted Tape Inserts, *International Journal of Thermal Sciences, 99* (2016), Jan., pp. 238-257

[19] Chen, J., *et al.*, Heat Transfer Enhancement in Dimpled Tubes, *Applied Thermal Engineering, 21* (2011), 5, pp. 535-547

[20] Vicente, P. G., *et al.*, Experimental Study of Mixed Convection and Pressure Drop in Helically Dimpled Tubes for Laminar and Transition Flow, *International Journal of Heat and Mass Transfer, 45* (2002), 26, pp. 5091-5105

[21] Mengna, H., *et al.*, Compound Heat Transfer Enhancement of a Converging–Diverging Tube with Evenly Spaced Twisted-Tapes, *Chinese Journal of Chemical Engineering, 15* (2007), 6, pp. 814-820

[22] Sivashanmugam, P., Suresh, S., Experimental Studies on Heat Transfer and Friction Factor Characteristics of Laminar Flow Through a Circular Tube Fitted with Helical Screw-Tape Inserts, *Applied Thermal Engineering, 26* (2006), 16, pp. 1990-1997

[23] Biswas, G., *et al.*, Augmentation of Heat Transfer by Creation of Streamwise Longitudinal Vortices using Vortex Generators, *Heat Transfer Engineering, 33* (2012), 4, pp. 406-424

[24] Kumar, P., *et al.*, Heat Transfer Enhancement in Short Corrugated Mini-Tubes, in: *Numerical Analysis of Heat and Mass Transfer in Porous Media*, (Eds. Delgado, J. M. P. Q., *et al.*), Advanced Structured Materials, Springer, New York, USA, 2012, Vol. 27, pp. 181-208

[25] Li, B., *et al.*, Experimental Study on Friction Factor and Numerical Simulation on Flow and Heat Transfer in an Alternating Elliptical Axis Tube, *Applied Thermal Engineering, 26* (2006), 17-18, pp. 2336-2344

[26] Saha, S. K., *et al.*, Enhancement of Heat Transfer of Laminar Flow of Viscous Oil through a Circular Duct Having Integral Axial Rib Roughness and Fitted with Helical Screw-Tape Inserts, *Heat Transfer Research, 43* (2012), 3, pp. 207-227

[27] Bhattacharyya, S., *et al.*, Numerical Study on Heat Transfer Enhancement through a Circular Duct Fitted with Centre-Trimmed Twisted Tape, *International Journal of Heat and Technology, 34* (2016), 3, pp. 401-406

[28] Benim, A. C., A Finite Element Solution of Radiative Heat Transfer in Participating Media Utilizing the Moment Method, *Computer Methods in Applied Mechanics and Engineering, 67* (1988), 1, pp. 1-14

[29] ***, ANSYS Fluent User Manual, www.ansys.com

[30] Assmann, A., *et al.*, Pulsatile Extracorporeal Circulation During On-Pump Cardiac Surgery Enhances Aortic Wall Shear Stress, *Journal of Biomechanics, 45* (2012), 1, pp. 156-163

[31] Abraham, J. P., *et al.*, Heat Transfer in All Pipe Flow Regimes: Laminar, Transitional/Intermittent, and Turbulent, *International Journal of Heat and Mass Transfer, 52* (2009), 3-4, pp. 557-563

[32] Oclon, P., *et al.*, Numerical Study on the Effect of Inner Tube Fouling on the Thermal Performance of High-Temperature Fin-and-Tube Heat Exchanger, *Progress in Computational Fluid Dynamics – An International Journal, 15* (2015), 5, pp. 290-306

[33] Bhattacharyya, S., *et al.*, Convective Heat Transfer Enhancement and Entropy Generation of Laminar Flow of Water through a Wavy Channel, *International Journal of Heat and Technology, 34* (2016), 4, pp. 727-733

[34] Kadiyala, P. K., Chattopadhyay, H., Numerical Analysis of Heat Transfer from a Moving Surface Due to Impingement of Slot Jets, *Heat Transfer Engineering, 39* (2017), 2, pp. 1-9

[35] Bhattacharyya, S., *et al.*, Simulation of Heat Transfer Enhancement in Tube Flow with Twisted Tape Insert, *Progress in Computational Fluid Dynamics - An International Journal, 17* (2017), 3, pp. 193-197

[36] Bhattacharyya, S., *et al.*, Computational Investigation of Heat Transfer Enhancement by Alternating Inclined Ribs in Tubular Heat Exchanger, *Progress in Computational Fluid Dynamics - An International Journal, 17* (2017), 6, pp. 390-396

[37] Bhattacharyya, S., *et al.*, Investigation of Inclined Turbulators for Heat Transfer Enhancement in a Solar Air Heater, *Heat Transfer Engineering*, On-line first, https://doi.org/10.1080/01457632.2018.1474593, 2018